Acta Crystallographica Section D
Biological Crystallography
ISSN 0907-4449

Crystallization, structure solution and refinement of hen egg-white lysozyme at pH 8.0 in the presence of MPD

Manfred S. Weiss,*† Gottfried J. Palm† and Rolf Hilgenfeld

Institute of Molecular Biotechnology, Department of Structural Biology and Crystallography, PO Box 100813, D-07708 Jena, Germany

† MSW and GJP contributed equally to this work.

Correspondence e-mail: msweiss@imb-jena.de

Received 5 January 2000
Accepted 3 May 2000

PDB References: MPD form, 1dpw; NaCl form, 1dpx.

Hen egg-white lysozyme has been crystallized at slightly alkaline pH using 2-methyl-2,4-pentanediol (MPD) as the precipitant. The crystals are nearly isomorphous to crystals grown at acidic pH using sodium chloride as the precipitant. However, the growth kinetics differ markedly between the two conditions. The major reason for this is a molecule of MPD that binds tightly in between two lysozyme molecules and favors the growth of the crystals along the crystallographic *c* direction over growth perpendicular to it.

1. Introduction

Hen egg-white lysozyme (E.C. 3.2.1.17; HEWL) was the first enzyme to have its three-dimensional structure determined (Blake *et al.*, 1965, 1967) and has become one of the most studied enzymes in structural biology to date. The reason for this is that it can be easily crystallized in various crystal forms which yield X-ray diffraction data to high resolution and in high quality.

Five different space groups of HEWL crystals with seven different unit cells occur among the 62 native HEWL structures deposited as of July 1999 in the PDB (Bernstein *et al.*, 1977) and 14 different crystallization conditions are reported in the Biological Macromolecule Crystallization Database (BMCD) at NIST (Gilliland *et al.*, 1994). Of these 14 conditions, five are at alkaline pH, but in only one of these five cases was the tetragonal space group $P4_32_12$ with unit-cell parameters $a = 78.9$, $c = 38.5$ Å obtained. However, these crystals grew from an isoionic solution of HEWL sulfate (Riès-Kautt *et al.*, 1994). Recently, Forsythe *et al.* (1999) also reported crystallization of HEWL at alkaline pH in the presence of sulfates. All other conditions, including those where a combination of high pH with an organic solvent was used, yielded different crystal lattices. In another recent report, however, commercially available lysozyme which had been additionally purified by cation-exchange chromatography yielded tetragonal crystals at pH values of up to 8.6 in the presence of NaCl (Ewing *et al.*, 1996). Above pH 7.4, unpurified material yielded only needles or rods, the space group of which could not be determined owing to their small size.

Here, we report the crystallization of HEWL in its tetragonal space group at alkaline pH using the organic solvent 2-methyl-2,4-pentanediol (MPD) as a precipitant, the structure solution and the refinement. The structure of the protein in complex with one molecule of MPD is described in detail, as are the differences to the structure of HEWL at pH 4.5 in the presence of NaCl.

2. Materials and methods

Commercially available hen egg-white lysozyme (Merck; Product No. 5282.0001, Lot No. K00504782) was used for crystallization without further purification. The lyophilized material was dissolved in deionized water to a concentration of 30 mg ml^{-1}. For crystallization at pH 4.5, a 5 µl drop of protein solution was mixed with an equal volume of reservoir solution containing 50 m*M* sodium acetate buffer at pH 4.5 and 5%(*w*/*v*) NaCl. The hanging drop was then equilibrated against this reservoir at room temperature. For crystallization at pH 8.0, the reservoir solution contained 50 m*M* tris(hydroxymethyl)aminomethane (Tris) pH 8.0 and 70%(*v*/*v*) MPD in water.

For data collection, the crystals were flash-cooled in a nitrogen stream at a temperature of 100 K. The MPD crystal form was flash-cooled without any further cryoprotective treatment, whereas for the NaCl crystal form paraffin oil (Merck, highly liquid, No. 7174) was used as a cryoprotectant (Riboldi-Tunnicliffe & Hilgenfeld, 1999). Complete data sets of comparable redundancies were collected from both crystals using Cu $K\alpha$ radiation produced by an FR591 rotating-anode generator (Nonius, Delft, The Netherlands) operated at 40 kV and 90 mA and equipped with a 30 cm imaging-plate system (MAR Research, Hamburg, Germany). In both cases, severe ice formation on the goniometer head and on the crystal made frequent interruption of the data collection necessary in order to clean the crystals from growing ice. For the NaCl crystal form, a total of 180° of data were collected and for the MPD crystal form the total rotation range was 212°. The data were processed using the program *DENZO* (Otwinowski, 1993) and were scaled and merged using *SCALEPACK* (Otwinowski, 1993). The redundancy-independent merging *R* factor $R_{\rm r.i.m.}$ (Weiss & Hilgenfeld, 1997; Diederichs & Karplus, 1997) as well as the precision-indicating merging *R* factor $R_{\rm p.i.m.}$ (Weiss & Hilgenfeld, 1997) were calculated based on scaled but unmerged intensity values as output by *SCALEPACK* (option NO MERGE ORIGINAL INDEX) using our own program (available from the internet at http://www.imb-jena.de/www_sbx/projects/sbx_qual.html or from the authors upon request). Intensities were converted to structure factors using the method of French & Wilson (1978) as implemented in the program *TRUNCATE* (Collaborative Computational Project, Number 4, 1994).

The structure was solved using PDB entry 1hel (resolution 1.7 Å, *R* factor = 15.2%; Wilson *et al.*, 1992) as a starting model. The position and orientation of the protein in the slightly smaller unit cell was adjusted by rigid-body refinement using the program *REFMAC* (Collaborative Computational Project, Number 4, 1994). The structure was then refined at high resolution using a maximum-likelihood target function as implemented in the program *REFMAC* (Collaborative Computational Project, Number 4, 1994). Refinement cycles were iterated with automated water-building cycles using the program *ARP* (Lamzin & Wilson, 1993). After ten cycles, the structure was checked using a computer-graphics system, rebuilt in some places and further refinement was carried out

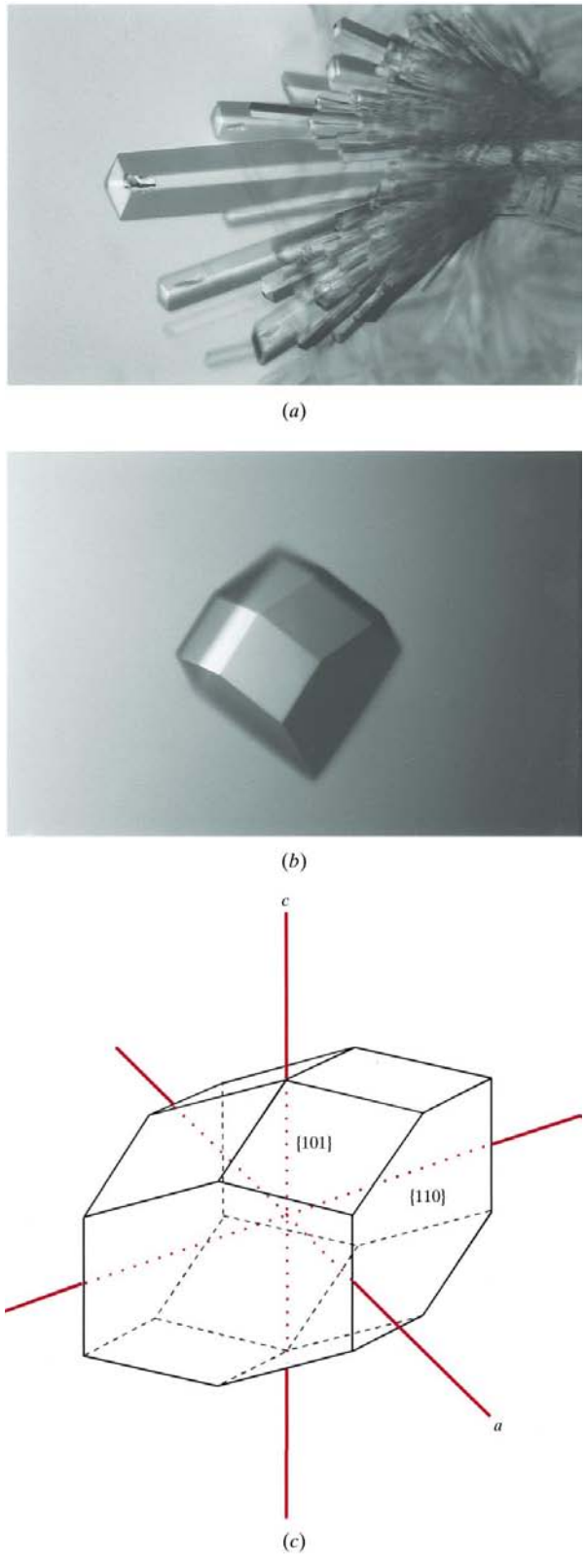

Figure 1
Photograph of a typical hen egg-white lysozyme crystal (*a*) grown at pH 8.0 using MPD as a precipitant and (*b*) grown at pH 4.5 in the presence of NaCl as a precipitant. In (*c*) the canonical crystal habit of the tetragonal space group with the {110} and the {101} faces developed is shown schematically. The crystallographic unit-cell axes are also indicated.

until convergence was reached. All graphics work was performed using the program *O* (Jones *et al.*, 1991) and all structure comparisons were carried out using the program *LSQKAB* (Collaborative Computational Project, Number 4, 1994), which is based on the vector-superposition algorithm of Kabsch (1978).

The buried accessible surface areas for the crystal contact areas were calculated with the program *GRASP* (Nicholls *et al.*, 1991). These areas were taken as the sum of the solvent-accessible surface areas of the two isolated molecules involved in forming the contact, less the solvent-accessible surface area of the combined pair of molecules. All solvent molecules except for the MPD were deleted from the coordinates for the calculation of the surface areas. The coordinate and structure-factor sets of both the MPD and the NaCl crystal forms have been deposited with the PDB.

3. Results and discussion

The lysozyme crystals obtained at pH 8.0 in the presence of MPD are shown in Fig. 1(*a*). For comparison, a crystal grown at pH 4.5 in the presence of NaCl as precipitant is shown in Fig. 1(*b*). Even though the crystal habit of the MPD crystal form looks very different from that of the NaCl crystal form at first sight, the crystals belong to the same space group, $P4_32_12$, with almost the same unit-cell parameters. In the pH 8.0 MPD crystals the bipyramidal {101} faces appear to be retained, whereas the prismatic {110} faces appear to be replaced by {100} faces. A control experiment using the same material and setup did not yield crystals when the pH was raised above 5.0 and NaCl was used as the precipitant or when the pH was lowered below 7.0 and MPD was used as the precipitant. This finding is in contrast to results obtained by Ewing *et al.* (1996), who reported successful crystallization of lysozyme at high pH in its tetragonal space group using NaCl as the precipitant. The combination of MPD and NaCl as precipitants also led to successful crystallization at pH 4.5 using the gel-crystallization method (PDB entry 1bvx; Dong *et al.*, 1999). In another recent report on the influence of additives on protein crystallization, no effect of MPD on the crystallization of HEWL at low pH was found (Sauter *et al.*, 1999). In the latter two cases, however, the MPD concentration in the crystallizing solution was 15%(*w*/*v*) or even less, so that the high concentration of NaCl present might have masked any effects of the MPD.

Some details of the data collection and processing are given in Table 1. From these it is evident that both collected data sets are of very high quality. Both crystals diffracted well beyond 1.6 Å resolution, but data were only collected to a maximum resolution of 1.64 Å owing to the detector setup. Both data sets have the same redundancy, therefore the data set for the NaCl crystal form appears to be of higher quality since it has the better merging statistics.

The refinement statistics are also listed in Table 1. Both structures are well refined with comparable deviations from ideal geometry. Interestingly, the data set of the MPD crystal form which exhibits somewhat inferior merging statistics yielded the better refinement results in terms of both a lower *R* factor and a lower free *R* factor. Also, fewer solvent molecules have been identified in the MPD crystal form. It is possible that a higher contrast in electron density between the protein region and the solvent region in the MPD crystal form compared with the NaCl crystal form led to the better refinement statistics. This notion is supported by the experience that crystals grown from polyethyleneglycol as a precipitant always seem to yield clearer maps in the protein region and less noise from the solvent region, but we are not aware of any systematic study in the literature that could support this hypothesis. A comparison of the two structures yields root-mean-square deviations of 0.22, 0.21 and 0.62 Å for the superposition of 129 C^{α} atoms, 514 main-chain atoms and all

Table 1
Data collection and refinement statistics.

	MPD crystal form	NaCl crystal form
Data collection		
Number of crystals	1	1
Total rotation range (°)	212	180
a (Å)	77.51	77.05
c (Å)	37.42	37.21
Resolution limits (Å)	100.0–1.64	100.0–1.65
Total number of reflections	183746	176694
Unique reflections	14454	13962
Redundancy	12.71	12.66
Completeness, overall (%)	99.7	99.7
Outer shell† (%)	100.0	100.0
$I/\sigma(I)$, overall	25.6	51.0
Outer shell†	14.6	19.4
$R_{\rm merge}$‡ (%)	8.0	3.8
Outer shell†(%)	19.0	14.3
$R_{\rm r.i.m.}$§ (%)	8.8	4.1
Outer shell† (%)	20.7	14.9
$R_{\rm p.i.m.}$¶ (%)	2.5	1.2
Outer shell† (%)	5.8	4.2
Overall *B* factor from Wilson plot (Å^2)	17.2	17.2
Refinement		
Resolution limits (Å)	40.0–1.64	40.0–1.65
Data cutoff [$F/\sigma(F)$]	0.0	0.0
Total no. of reflections	14451	13961
No. of reflections in working set	13723	13267
No. of reflections in test set	728	694
R†† (%)	17.83	18.74
$R_{\rm free}$ (%)	22.18	24.65
No. of amino-acid residues	129	129
No. of protein atoms	1005‡‡	1013§§
No. of chloride ions	2	2
No. of water molecules	125	177
No. of other solvent atoms	24	—
Average *B* factor of all atoms (Å^2)	19.0	19.4
Average *B* factor of protein atoms (Å^2)	17.4	18.0
R.m.s.d. bonds (Å)	0.011	0.010
R.m.s.d. angles (°)	2.3	2.2

† The resolution limits of the outer shell are 1.70–1.64 Å for the MPD crystal form and 1.71–1.65 Å for the NaCl crystal form. ‡ $R_{\rm merge} = \sum_{hkl}\sum_i|I_i(hkl) - \overline{I(hkl)}|/\sum_{hkl}\sum_i I_i(hkl)$, where (hkl) denotes the sum over all reflections and i the sum over all equivalent and symmetry-related reflections (Stout & Jensen, 1968). § $R_{\rm r.i.m.}$ is the redundancy-independent merging *R* factor (Weiss & Hilgenfeld, 1997), which is identical to the $R_{\rm meas}$ of Diederichs & Karplus (1997). $R_{\rm r.i.m.} = \sum_{hkl}[N/(N-1)]^{1/2}\sum_i|I_i(hkl) - \overline{I(hkl)}|/\sum_{hkl}\sum_i I_i(hkl)$, with N being the number of times a given reflection has been observed. ¶ $R_{\rm p.i.m.}$ is the precision-indicating merging *R* factor (Weiss & Hilgenfeld, 1997). $R_{\rm p.i.m.} = \sum_{hkl}[1/(N-1)]^{1/2}\sum_i|I_i(hkl) - \overline{I(hkl)}|/\sum_{hkl}\sum_i I_i(hkl)$. †† $R = \sum_{hkl}|F_{\rm obs} - kF_{\rm calc}|/\sum_{hkl}F_{\rm obs}$. ‡‡ The side chain of Asn59 (CB, CG, OD1, ND2) has been modelled in two conformations. §§ The following amino-acid side chains (atoms) have been modelled in two conformations: Lys1 (CE, NZ), Arg14 (CB, CG, CD, NE, CZ, NH1, NH2), Asn77 (CB, CG, OD1, ND2) and Ser85 (CB, OG). The C-terminal carboxylate group of Leu129 has been omitted from the coordinates.

998 atoms (excluding the C-terminal carboxylate group), respectively. This shows that the changes in the protein structure are small when only the main-chain atoms are considered. Eight side chains comprising a total of 44 atoms exhibit clearly different conformations. These are Asp18, Ile55, Arg61, Ile78, Asp101, Arg112, Arg125 and Arg128. They all show r.m.s.d. values of ≥ 2.0 Å upon superimposing the two structures. Of these, Arg61, Arg112 and Arg125 are highly mobile side chains, hence the differences are most likely not of any significance. Asp18 in the MPD crystal form makes a strong salt bridge to Arg128, whereas in the NaCl crystal form the two side chains are further apart. Asp101 in the MPD crystal form makes a hydrogen bond to the main-chain amide group of residue 103, whereas in the NaCl crystal form it points into the surrounding solvent. These two apparent differences can probably be explained by a difference in the dielectric properties of the solvent. In the MPD crystal form the dielectric constant of the solvent is considerably lower than in the NaCl crystal form, thus favoring polar interactions energetically. The only differences between the two forms that are not easily explained are the side-chain conformations of the hydrophobic residues Ile55 and Ile78. However, both are clearly supported by the electron-density maps of the two crystal forms. It is possible that the different dielectric properties of the two solutions can also cause the hydrophobic side chains to adjust. If these eight side chains exhibiting different conformations are excluded from the superposition, the r.m.s.d. value is decreased to 0.27 Å, a value which is only slightly higher than that for the main-chain atoms. This shows that the changes in the main-chain atom positions are negligible when the pH is increased from 4.5 to 8.0 and when the solvent is changed, but that some of the side chains of the molecule do undergo a significant change in conformation.

Both structures were also compared to the PDB entry 193l (Vaney *et al.*, 1996), which is the highest resolution structure of HEWL in its tetragonal NaCl crystal form in the PDB to date (1.33 Å). This structure was solved and refined based on data collected at 279 K. The comparison yielded r.m.s.d. values of 0.25, 0.31 and 0.74 Å for the C^{α} atoms, the main-chain atoms and all atoms of the MPD crystal form, respectively, and 0.25, 0.25 and 0.76 Å for the respective atoms of the NaCl crystal form. These values are slightly higher but in general very similar and still in the range of the overall coordinate errors of the structures, showing that even the large difference in temperature does not have any strong influence on the overall structure of HEWL.

Two chloride ions were identified in the structure based on the observation that the temperature factors of water molecules in these positions refined to abnormally low values. In other studies, up to eight anion-binding sites and one cation-binding site were identified in HEWL crystals grown from NaCl (Lim *et al.*, 1998; Dauter *et al.*, 1999; Dauter & Dauter, 1999). The two chloride positions observed in our case correspond to the positions of the two chloride ions with the lowest temperature factors in the PDB entry 1lz8 (Dauter *et al.*, 1999). Since we did not add any additional chloride to the crystallizing solution, we presume that the batch of HEWL used for our study contained sufficient chloride ions in the first place. Water molecules have been located at the other six chloride positions identified by Dauter *et al.* (1999) and at the sodium position. None of these waters exhibit abnormally low temperature factors. It is possible, however, that these water positions constitute partially occupied ion-binding sites. The chloride site identified as early as 1967 by Blake *et al.* (1967) between the side chain of Arg114 and the main-chain amide N atom of Ser24 is occupied by a water molecule (HOH8, see Fig. 3) in our case. It is unlikely that this site constitutes a chloride site as can be judged from the rather small hydrogen-bonding distances in both the MPD form crystals and the NaCl form crystals. Also, based on anomalous intensity differences, Dauter *et al.* (1999) did not propose a chloride ion at this site.

Early in the refinement of the two structures it became clear that a molecule of MPD was bound between two lysozyme molecules in the MPD crystal form. This molecule is very well defined, with an average temperature factor for the eight MPD atoms of only 21.1 $Å^2$, which is only slightly higher than the average temperature factor for the protein atoms (17.4 $Å^2$). The stereochemical configuration at the 4-position of MPD is clearly *R* and the two dihedral angles defining the conformation of the (4*R*)-MPD exhibit nearly ideal *trans* values of 176° (C1—C2—C3—C4) and 179° (C2—C3—C4—C5). This is the most common conformation for (4*R*)-MPD as found in a survey of 24 protein crystal structures from the PDB (see *Appendix A*). The final $(2F_{obs} - F_{calc})$ electron density is shown in Fig. 2. The MPD molecule is tightly bound to the surface of the protein and constitutes an integral part of the crystal lattice. There are also two Tris buffer molecules bound to the surface of the lysozyme molecules, but these are rather loosely bound, as indicated by their temperature factors, which are almost doubled compared with the temperature factors of the protein and the MPD atoms. In the recently reported structure of gel-crystallized HEWL where MPD was present in the crystallization medium (Dong *et al.*, 1999), no MPD molecule was found to bind to lysozyme (Dong, Helliwell & Olczak, personal communication). However, in this case the crystals were grown at pH 4.5 and the concentration of MPD used was much lower. This suggests that MPD may only be able to bind to lysozyme at high pH values and/or at high concentrations.

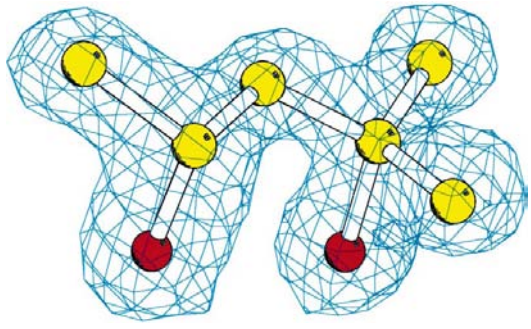

Figure 2
The conformation of the MPD molecule superimposed on the final $(2F_{obs} - F_{calc})$ electron density contoured at 1.0 standard deviations above the mean.

The MPD-binding site lies on the surface of one molecule at the entrance to the active site. However, it is not anywhere near the sugar moieties observed in the structure of the D25S mutant of HEWL in complex with tetra-*N*-acetyl chitotetraose (PDB entry 1lsz; Hadfield *et al.*, 1994). The closest distance from the MPD to the binding site of this carbohydrate is approximately 10 Å. The part of the protein that is involved in making contacts to the MPD molecule is the C-terminal end of the second α-helix in the structure plus (indirectly) the side chain of Arg114. From the other molecule, the loop between the first two α-helices comprising residues 17–24 contains the atoms that contact the MPD. The MPD does not occupy any of the minor anion-binding sites which were observed by Dauter *et al.* (1999). However, MPD binds in the neighborhood of the chloride Cl208 (PDB entry 1lz8), with the closest distance being about 3.5 Å between C1 of the MPD and the chloride ion. That means that MPD binding does not interfere with chloride binding at this position sterically. As a matter of fact, electron density has been observed at the corresponding position in our crystal form, but assigned to a water molecule (HOH29).

The environment of the MPD molecules in the crystal lattice is shown schematically in Fig. 3(*a*). The crystallographic symmetry operator which relates the two molecules between which the MPD is bound is $(-y+\frac{1}{2}, x+\frac{1}{2}, z-\frac{1}{4})$. There is only one direct hydrogen bond between the O2 of the MPD and the Phe34 O atom of the reference molecule and one to the Gly22 O atom of the symmetry-related molecule. As can be seen from Fig. 3(*a*), there are many more interactions between these two molecules bridged by water molecules. For comparison, the situation in the NaCl crystal form is shown in Fig. 3(*b*). Instead of the MPD molecule, there are two water molecules bound. The two other water molecules that are present in the MPD crystal form (HOH191 and HOH193) are not present in the NaCl crystal form. In summary, the NaCl crystal form contains four fewer direct or water-bridged polar interactions across this crystal contact than the MPD crystal form.

An overall view of the unit cell and of the two lysozyme molecules related by the symmetry operator $(-y+\frac{1}{2}, x+\frac{1}{2}, z-\frac{1}{4})$ is shown in Fig. 4 together with the MPD-binding site in between these two molecules. Since the MPD contacts two molecules in the crystal lattice, it is conceivable that it has

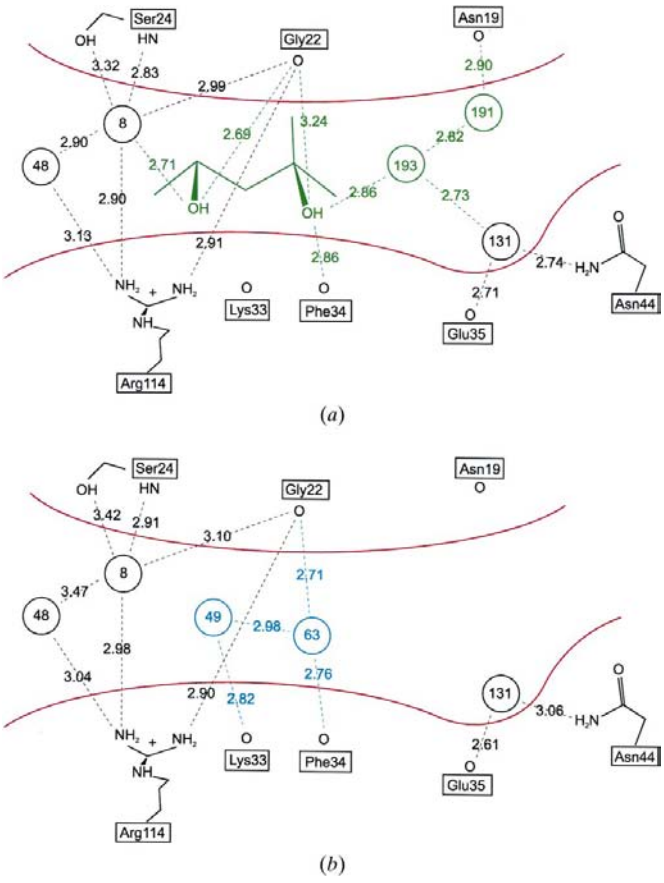

Figure 3
Schematic representation of (*a*) the MPD-binding site in the MPD crystal form and (*b*) the same site in the NaCl crystal form. The circles with numbers in constitute bound water molecules. All polar contacts ≤ 3.5 Å are shown at this interface. The distances of the respective interactions are given in Å. The coloured lines denote the interactions which are only present in one crystal form, whereas the black lines denote interactions that are present in both forms. It is clearly discernible that the MPD contributes to the total interaction surface between the two HEWL molecules.

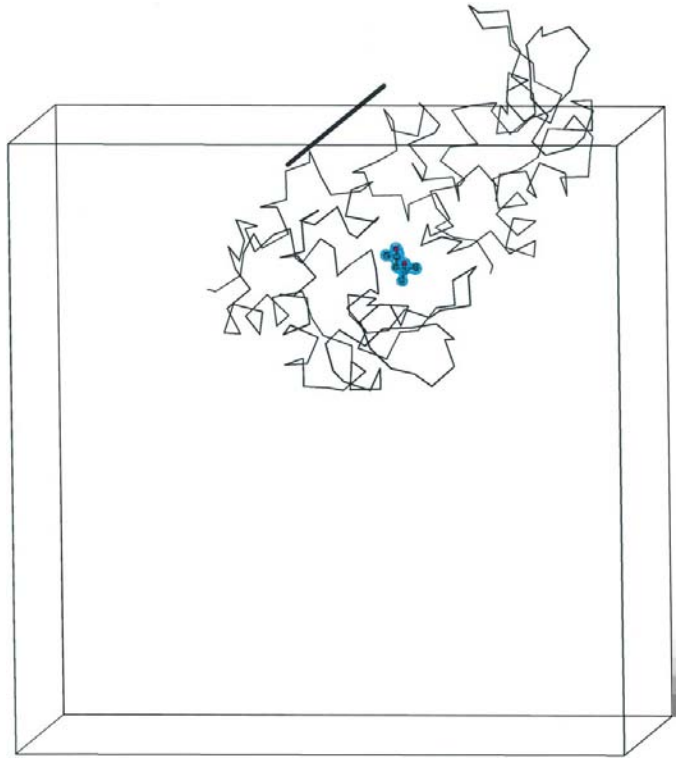

Figure 4
Packing of the lysozyme monomers in the tetragonal crystal form. The view is approximately down the *c* axis of the unit cell. Two molecules are shown as C^{α} traces. The two molecules are related by the symmetry operator $(-y+\frac{1}{2}, x+\frac{1}{2}, z-\frac{1}{4})$. The MPD-binding site between these two molecules is indicated by the electron density and the ball-and-stick representation of the MPD molecule. The 4_3 screw axis which relates the two molecules drawn is shown as a thick line.

some influence on the growth kinetics of the crystal and therefore on the crystal habit. A list of the crystal contact areas, the number of atomic contacts $\leq$3.5 Å between molecules and the buried surface areas upon contact formation are given in Table 2. A total of six surface areas on each protein molecule are involved in crystal contact formation. These six areas can be described by four different symmetry operators which leaves two isologous contacts (Monod *et al.*, 1965) around crystallographic twofold axes (contact areas I and II) and two heterologous contacts (Monod *et al.*, 1965) along a crystallographic twofold screw axes (contact areas III and IV). According to Wukovitz & Yeates (1995), the minimal number of necessary contacts in space group $P4_32_12$ is two. It can be easily derived that in our case the two largest contact areas I and II (see Table 2), which are the contacts that form HEWL dimers across a crystallographic twofold axis, are not sufficient to form the lattice. The contacts that connect these dimers in the crystal lattice are those represented by contact areas III or IV; at least one of them is needed to form the three-dimensional lattice. The minimal combination of contact areas are I + III or II + III or I + II + IV. Contact III connects the lysozyme monomers in a helix-like fashion around the crystallographic 4_3 axis (Fig. 4). It is this contact that is preferentially stabilized by the MPD molecule. The MPD also increases the buried surface area of this contact by about 100 Å^2, whereas at contact I the lysozyme molecules are slightly further apart in the MPD crystal form compared with the NaCl crystal form. This decreases the buried surface area of this contact by about 100 Å^2. These two main changes are probably responsible for the preferential growth of the MPD form crystals along the crystallographic *c* direction. A similar change in the crystal habit was reported when polyethylene glycols of molecular weights 1000 and 6000 were used as additives to HEWL crystallization at low pH, but no analysis on the molecular level was performed (Sauter *et al.*, 1999).

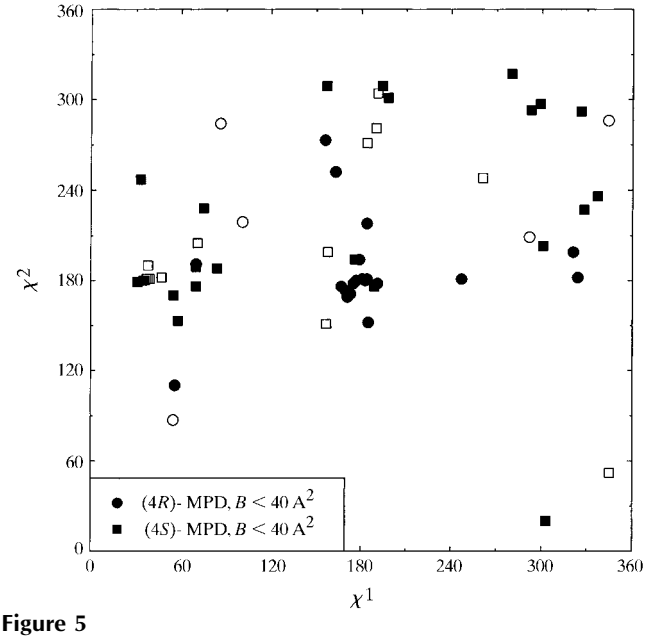

Figure 5
Conformation of MPD molecules for (4*R*)-MPD (circles) and (4*S*)-MPD (squares). Molecules with average *B* factors greater than 40 A^2 are designated by the respective open symbols. The favored regions are conformations with neighboring hydroxyl groups in (4*R*)-MPD ($\chi_1 = 180$, $\chi_2 = 180°$) and (4*S*)-MPD ($\chi_1 = 60$, $\chi_2 = 180°$), respectively.

Table 2
Crystal contact areas for tetragonal lysozyme crystals grown with MPD and NaCl.

Only atoms of the protein and the MPD molecule were used for these calculations. The C-terminal carboxyl group of the coordinate set in the MPD crystal form was deleted for these calculations in order to make the areas directly comparable between the two structures. In case of observed alternate conformations of side chains, both conformations were taken into consideration.

		MPD crystal form		NaCl crystal form	
	Symmetry operator	No. of contacts†	Buried surface area (Å^2)	No. of contacts†	Buried surface area (Å^2)
I	$y, x, -z + 1$	28	855	28	950
II	$-y, -x, -z + \frac{1}{2}$	20	1145	20	1135
III	$-y + \frac{1}{2}, x + \frac{1}{2}, z - \frac{1}{4}$; $y - \frac{1}{2}, -x + \frac{1}{2}, z + \frac{1}{4}$	20	665	15	565
IV	$-y + \frac{1}{2}, x + \frac{1}{2}, z + \frac{3}{4}$; $y - \frac{1}{2}, -x + \frac{1}{2}, z - \frac{3}{4}$	3	375	8	400

† Only contacts with distances of $\leq$3.5 Å were taken into account.

What remains completely unclear is why the MPD crystal forms grows solely at alkaline pH and the NaCl crystal form grows preferentially at acidic pH. The MPD-binding site contains no residue that would change its protonation state between these two conditions. However, at acidic pH and a MPD concentration of about 15%, no MPD is bound to the surface of lysozyme (Dong *et al.*, 1999; Dong, Helliwell & Olczak, personal communication). This means that it is either the higher pH that allows the MPD to bind to the protein or the higher concentration of the MPD in solution that enforces the association. The tight binding of the MPD (five hydrogen bonds compared with 2.2 on average in other protein/MPD complex structures; see *Appendix A*) and the fact that we could not obtain crystals at acidic pH when MPD was the only precipitant stress the importance of the pH. Therefore, at high pH a complex between MPD and HEWL might form, which then crystallizes. This notion, however, is merely speculative at this time and must await further experimental clarification. In a survey of MPD molecules bound to protein crystal structures (see *Appendix A*), however, no influence of the pH of the crystallization solution on the binding of MPD to proteins in general could be detected.

4. Conclusions

We have reported the growth of tetragonal hen egg-white lysozyme crystals at alkaline pH in the presence of MPD. The structure revealed that one MPD molecule is bound in the crystal lattice between two lysozyme molecules. This MPD molecule strengthens one of the crystal contacts relative to the others, leading to a different growth behaviour and therefore a different crystal habit.

APPENDIX *A*

As a common precipitant, MPD has been described as part of the solvent structure in a number of entries in the PDB and the Cambridge Structural Database (CSD). We have used 58 crystallographically independent MPD molecules from 24 PDB entries (1ad2, 1afw, 1bf6, 1byz, 1cxl, 1d3c, 1dpw, 1lam, 1lcp, 1lgc, 1mkp, 1moq, 1nco, 1qbz, 1rpg, 1sfc, 1swu, 2mcm, 2sn3, 2trx, 3al1, 4bp2, 4fab, 5adh) to analyze crystallization conditions and hydrogen-bonding partners. Adding seven occurrences from five CSD entries (BACXIM, KOFPAW, NIRQIO, NOSVOG, TECYIJ), we have also checked the MPD conformation.

A1.1. Crystallization conditions. The pH distribution of the crystallization conditions for the mentioned PDB entries is very similar to that for all BMCD entries, with most pH values between 6.0 and 8.0. The MPD concentration used was mostly 50–70%.

A1.2. Configuration and conformation. For structural analysis we have used the coordinates as given, even though the assignment of the O and C atoms and therefore the stereochemistry and χ angles are ambiguous in some cases. Both configurations of MPD are observed [(4*R*), 26 times; (4*S*), 39 times]. The distribution of the dihedral angles χ_1 [C1(proR)—C2—C3—C4] and χ_2 (C2—C3—C4—C5) is not random (Fig. 5). Firstly, χ angles of 60, 180 and 300° are preferred, as expected. Secondly, conformations with two short 1–5 distances [$\chi_2 = 300°$ for (4*R*)-MPD, $\chi_2 = 60°$ for (4*S*)-MPD] are disfavoured. Thirdly, all other conformations exhibit only one short 1–5 distance; out of these, the conformation with the two hydroxyl groups being in close contact is the most favoured [$\chi_1 = 180°$, $\chi_2 = 180°$ for (4*R*)-MPD; $\chi_1 = 60°$, $\chi_2 = 180°$ for (4*S*)-MPD]. This conformation is also observed in the above described structure.

A1.3. Hydrogen bonding. The two hydroxyl groups of MPD have the same hydrogen-bonding partners (cutoff at 3.5 Å), preferably water molecules (44%), main-chain O atoms (18%) and side-chain atoms of Arg, Lys, Glu, Asp, Ser and Thr (28%). On average, 2.2 hydrogen bonds are made per MPD molecule. Nine MPD molecules (in 1byz, 1dpw, 1rpg, 2mcm, 2sn3, 2trx, 3ali, 4bp2) contact two peptide chains either directly or *via* water molecules.

We would like to thank Ulrike Gröbner for her help in growing the crystals. This work was carried out within the European Bio-Crystallogenesis Initiative and supported by the European Commission (Grant #BIO4-CT98-0086). RH thanks the Fonds der Chemischen Industrie for support.

References

Bernstein, F. C., Koetzle, T. F., Williams, G. J. B., Meyer, E. F. Jr, Brice, M. D., Rodgers, J. R., Kennard, O., Shimanouchi, T. & Tasumi, M. (1977). *J. Mol. Biol.* **112**, 535–542.
Blake, C. C. F., Koenig, D. F., Mair, G. A., North, A. C. T., Phillips, D. C. & Sarma, V. R. (1965). *Nature (London)*, **206**, 757–761.
Blake, C. C. F., Mair, G. A., North, A. C. T., Phillips, D. C. & Sarma, V. R. (1967). *Proc. R. Soc. London B*, **167**, 365–377.
Collaborative Computational Project, Number 4 (1994). *Acta Cryst.* D**50**, 760–763.
Dauter, Z. & Dauter, M. (1999). *J. Mol. Biol.* **289**, 93–101.
Dauter, Z., Dauter, M., de La Fortelle, E., Bricogne, G. & Sheldrick, G. M. (1999). *J. Mol. Biol.* **289**, 83–92.
Diederichs, K. & Karplus, P. A. (1997). *Nature Struct. Biol.* **4**, 269–275.
Dong, J., Boggon, T. J., Chayen, N. E., Raftery, J., Bi, R.-C. & Helliwell, J. R. (1999). *Acta Cryst.* D**55**, 745–752.
Ewing, F. L, Forsythe, E. L., van der Woerd, M. & Pusey, M. L. (1996). *J. Cryst. Growth*, **160**, 389–397.
Forsythe, E. L., Snell, E. H., Malone, C. C. & Pusey, M. L. (1999). *J. Cryst. Growth*, **196**, 332–342.
French, G. S. & Wilson, K. S. (1978). *Acta Cryst.* A**34**, 517--525.
Gilliland, G. L., Tung, M., Blakeslee, D. M. & Ladner, J. (1994). *Acta Cryst.* D**50**, 408–413.
Hadfield, A. T., Harvey, D. J., Archer, D. B., MacKenzie, D. A., Jeenes, D. J., Radford, S. E., Lowe, G., Dobson, C. M. & Johnson, L. N. (1994). *J. Mol. Biol.* **243**, 856–872.
Jones, T. A., Zou, J. Y., Cowan, S. W. & Kjeldgaard, M. (1991). *Acta Cryst.* A**47**, 110–119.
Kabsch, W. (1978). *Acta Cryst.* A**34**, 827–828.
Lamzin, V. S. & Wilson, K. S. (1993). *Acta Cryst.* D**49**, 129–149.
Lim, K., Nadarajah, A., Forsythe, E. L. & Pusey, M. (1998). *Acta Cryst.* D**54**, 899–904.
Monod, J., Wyman, J. & Changeux, J. P. (1965). *J. Mol. Biol.* **12**, 88–118.
Nicholls, A., Sharp, K. & Honig, B. (1991). *Proteins*, **11**, 281–296.
Otwinowski, Z. (1993). *Proceedings of the CCP4 Study Weekend. Data Collection and Processing*, edited by L. Sawyer, N. Isaacs & S. Bailey, pp. 56–62. Warrington: Daresbury Laboratory.
Riboldi-Tunnicliffe, A. & Hilgenfeld, R. (1999). *J. Appl. Cryst.* **32**, 1003–1005.
Riès-Kautt, M., Ducruix, A. & Van Dorsselaer, A. (1994). *Acta Cryst.* D**50**, 366–369.
Sauter, C., Ng, J. D., Lorber, B., Keith, G., Brion, P., Hosseini, M. W., Lehn, J.-M. & Giegé, R. (1999). *J. Cryst. Growth*, **196**, 365–370.
Stout, G. H. & Jensen, L. H. (1968). *X-ray Structure Determination. A Practical Guide*, p. 402. London: Macmillan.
Vaney, M. C., Maignan, S., Riès-Kautt, M. & Ducruix, A. (1996). *Acta Cryst.* D**52**, 505–517.
Weiss, M. S. & Hilgenfeld, R. (1997). *J. Appl. Cryst.* **30**, 203–205.
Wilson, K. P., Malcolm, B. A. & Matthews, B. W. (1992). *J. Biol. Chem.* **267**, 10842–10849.
Wukovitz, S. Z. & Yeates, T. O. (1995). *Nature Struct. Biol.* **2**, 1062–1067.